Supplementary Figure S1

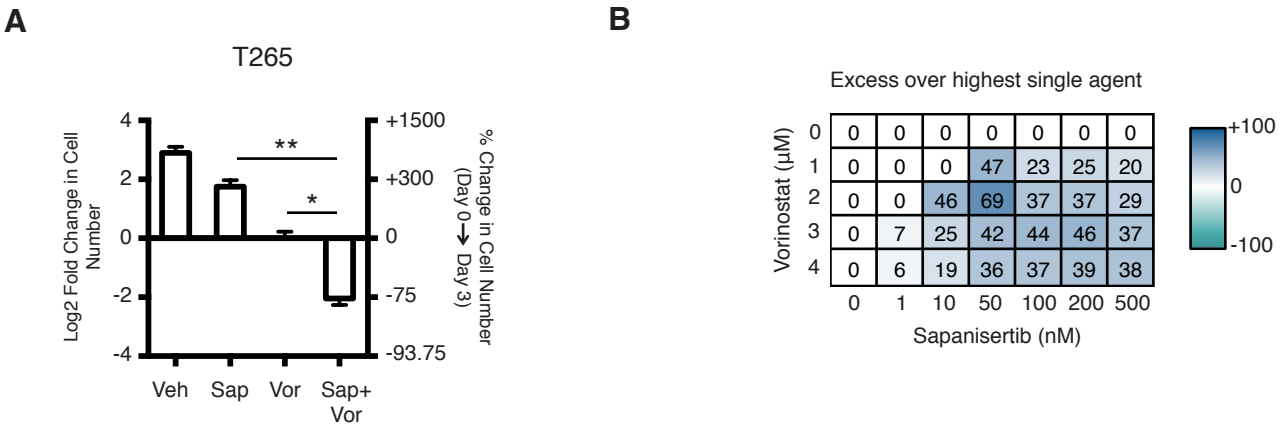

Supplementary Figure S1. MPNSTs are sensitive to combined HDAC and mTOR inhibtion. **A)** p53 WT MPNST cell line T265 was treated with vehicle (veh), sapanisertib (200nM, sap), vorinostat (2μM, vor), or vorinostat and sapanisertib (200nM) for 3 days. Left y-axis indicates log 2 of fold change in cell number at 3 days relative to day 0. Right y-axis indicates percent change in cell number at 3 days on a log 2 scale. Error bars ±SD from technical triplicates. Two other p53 WT MPNST cell lines (88-14 and SNF96.2) were also sensitive to the this combination (data not shown). **B)** Vorinostat and sapanisertib are synergistic according to Gaddum's non-interaction model, which is the most appropriate model for assessing synergy on cytotoxicity when at least one agent (sapanisertib) is purely cytostatic. 90-8TLs were treated with indicated drug concentrations for three days and viability was assessed by cell titer glow. The percent decrease in viability realtive to day 0 was calculated as a proxy for cell death. The excess over the highest single agent was calculated and is shown in the matrix, with 100 indicating complete synergy, and -100 indicating complete antagonism. Boxes are shaded according to the color scale shown. *p=0.000006, **p<0.000001

Supplementary Figure S2

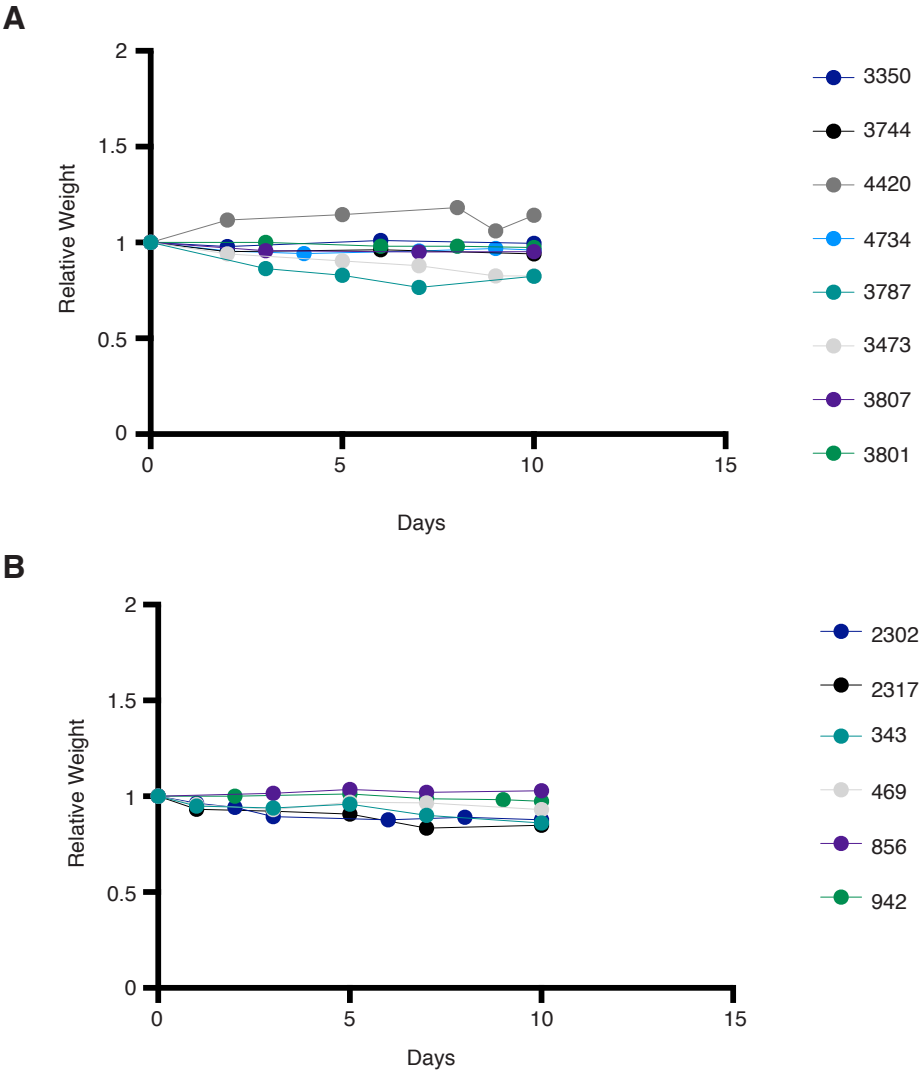

Supplementary Figure S2. Change in animal weight while on combiniation treatment. **A)** Weight of same animals in Figure 1G treated with rapamycin and vorinostat. Y-axis indicates relative weight (normalized to day 0 weight of individual animal). X-axis indicates days on treatment. Legend at right shows mouse number of each mouse. **B)** Weight of same animals in Figure 1J treated with sapanisertib and panobinostat. Y-axis indicates relative weight (normalized to day 0 weight of individual animal). X-axis indicates days on treatment. Legend at right shows mouse number of each mouse.

Supplementary Figure S3

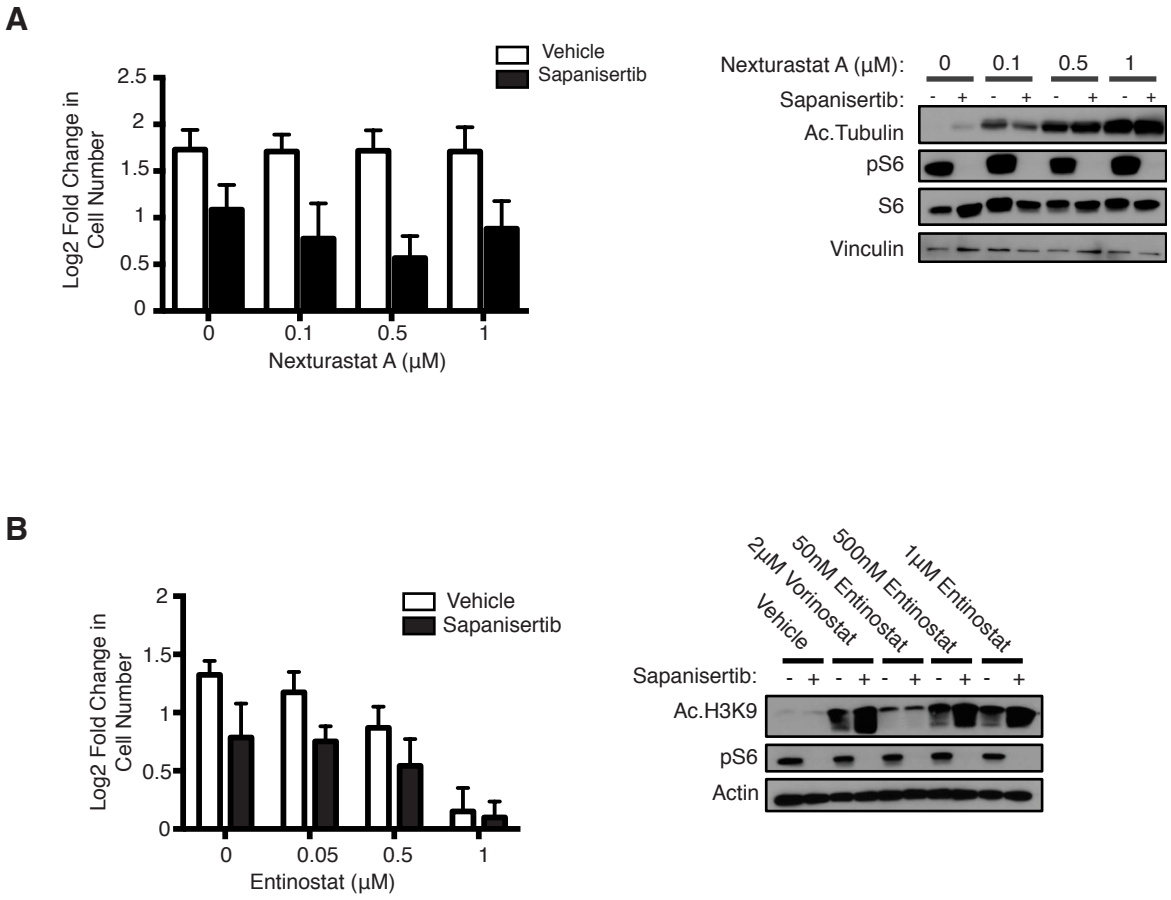

Supplementary Figure S3. **A)** 90-8TL cells were treated with Nexturastat A at concentration indicated, with (black) or without (white) 100nM sapanisertib. Graph depicts the mean log2 fold change of cell number after 72 hours, relative to day 0 ±SD. At right, immunoblots depict acetylated lysine 9 on histone H3 (Ac. H3K9) and phosphorylated S6 (pS6). Total S6 and vinculin serve as a loading controls. **B)** 90-8TLs were treated with entinostat at indicated concentrations, with (black) or without (white) 100nM sapanisertib. At right, immunoblots depict acetylated lysine 9 on histone H3 (Ac. H3K9) and phosphorylated S6 (pS6). Actin serves as a loading control.

Supplementary Figure S4

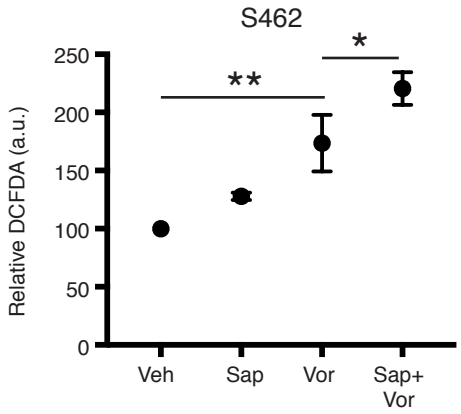

Supplementary Figure S4. Combined HDAC and mTOR inhibition increases reactive oxygen species in MPNSTs. **A)** Graph depicts relative mean fluorescence intensity of S462 cells stained with dichlorofluorescin diacetate (DCFDA), a dye that measures reactive oxygen species (ROS) and treated with vehicle (veh), sapanisertib (sap), vorinostat (vor), or vorinostat and sapanisertib (sap + vor) for 24 hours. Error bars indicate SD from three technical triplicates. *p=0.007277, **p=0.000441

Supplementary Figure S5

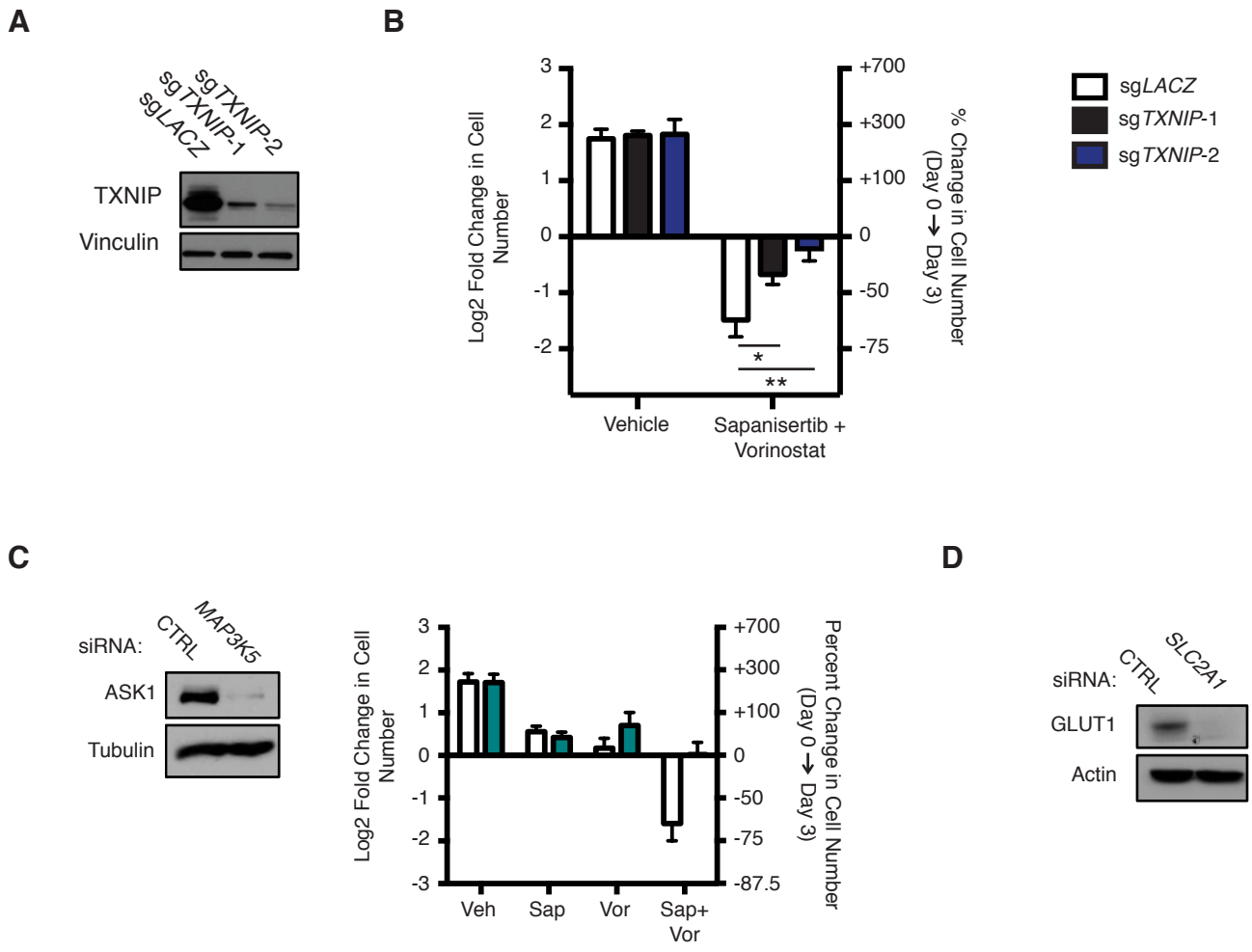

Supplementary Figure S5. TXNIP is required for combination induced MPNST cell death. **A)** 90-8TLs were infected with lentiCRISPRv2 expressing guides targeting *LACZ* or *TXNIP* as indicated. Immunoblot of TXNIP levels after 16 hours of sapanisertib and vorinostat treatment. Vinculin serves as a loading control. **B)** As in A, 90-8TLs were infected with lentiCRISPRv2 expressing guides against *LACZ* or *TXNIP* as indicated and treated with sapanisertib and vorinostat. Left y-axis indicates the log2 of fold change in cell number after 3 days. The right y-axis indicates the percent change in cell number after 72 hours relative to day 0 on a log2 scale. Error bars indicate SD of technical triplicates. *p=0.016, **p=0.00413 **C)** 90-8TLs were transfected with pooled siRNAs targeting MAP3K5 (ASK1) or non-targeting (CTRL) and treated with vehicle, sapanisertib (100nM), vorinostat (2μM), or sapanisertib and vorinostat. Left y-axis indicates the log2 of fold change in cell number after 3 days. The right y-axis indicates the percent change in cell number after 72 hours relative to day 0 on a log2 scale. Error bars indicate SD of technical triplicates. Vehicle and combination data are reprinted from Fig. 3K for clarity. Immunoblot showing ASK1 in 90-8TLs 72 hours after transfection with indicated siRNA (*MAP3K5* is the gene name for ASK1). Tubulin serves as a control. This immunoblot is a control for the experiment shown in Fig. 3K. **D)** Immunoblot showing GLUT1 in 90-8TLs 72 hours after transfection with indicated siRNA (*SLC2A1* is the gene name for GLUT1). Tubulin serves as a control. This immunoblot is a control for the experiment shown in Fig. 3L.

Supplementary Table S1. Differentially expressed gene sets in MPNSTs treated with HDAC and mTOR inhibitors. To identify the pathways that were deregulated in response to vorinostat and rapamycin 90-8TLs were treated with vehicle, sapanisertib (100nM), vorinostat (2μM), or combined sapanisertib + vorinostat for 24 hours and a microarray analysis was performed. Recurrent pathway-related gene sets that were differentially expressed in the combination treated cells relative to the other treatment groups (vehicle and monotherapies) are shown. Gene sets were considered significant if they reached a nominal p-value of <0.005 in at least one of the Efron-Tibshirani GSA test, LS permutation test, or KS permutation test as in Figure 2A. Gene sets were considered recurrent if at least three related gene sets reached significance.

Oxidative Stress
CHUANG_OXIDATIVE_STRESS_RESPONSE_UP
CHUANG_OXIDATIVE_STRESS_RESPONSE_DN
WEIGEL_OXIDATIVE_STRESS_BY_TBH_AND_H2O2
GARGALOVIC_RESPONSE_TO_OXIDIZED_PHOSPHOLIPIDS_TURQUOISE_DN
KYNG_RESPONSE_TO_H2O2
GARGALOVIC_RESPONSE_TO_OXIDIZED_PHOSPHOLIPIDS_TURQUOISE_UP
MOOTHA_ROS
MOOTHA_FFA_OXYDATION
ER stress
REACTOME_UNFOLDED_PROTEIN_RESPONSE
REACTOME_ACTIVATION_OF_CHAPERONES_BY_IRE1_ALPHA
REACTOME_ACTIVATION_OF_CHAPERONE_GENES_BY_ATF6_ALPHA
REACTOME_ACTIVATION_OF_CHAPERONES_BY_ATF6_ALPHA
Senescence and aging
FRIDMAN_SENESCENCE_DN
TANG_SENESCENCE_TP53_TARGETS_DN
LY_AGING_MIDDLE_DN
LY_AGING_OLD_DN
LY_AGING_PREMATURE_DN
KYNG_NORMAL_AGING_UP
Hypoxia
HARRIS_HYPOXIA
WEINMANN_ADAPTATION_TO_HYPOXIA_DN
MENSE_HYPOXIA_UP
KRIEG_HYPOXIA_VIA_KDM3A
WEINMANN_ADAPTATION_TO_HYPOXIA_UP
FARDIN_HYPOXIA_11
ELVIDGE_HIF1A_AND_HIF2A_TARGETS_DN
ELVIDGE_HIF1A_TARGETS_DN
IFN
REACTOME_ANTIVIRAL_MECHANISM_BY_IFN_STIMULATED_GENES
SANA_RESPONSE_TO_IFNG_DN
DER_IFN_ALPHA_RESPONSE_UP
DER_IFN_BETA_RESPONSE_UP
DER_IFN_GAMMA_RESPONSE_UP
REACTOME_INTERFERON_GAMMA_SIGNALING
REACTOME_INTERFERON_ALPHA_BETA_SIGNALING
TNF
SANA_TNF_SIGNALING_UP
PID_TNFPATHWAY
PHONG_TNF_TARGETS_DN
PHONG_TNF_TARGETS_UP
TIAN_TNF_SIGNALING_NOT_VIA_NFKB
VEGF
WESTON_VEGFA_TARGETS
ABE_VEGFA_TARGETS_2HR
WESTON_VEGFA_TARGETS_12HR
HELLEBREKERS_SILENCED_DURING_TUMOR_ANGIOGENESIS
Viral infection
BROWNE_HCMV_INFECTION_20HR_DN
ZHU_CMV_24_HR_UP
ZHU_CMV_8_HR_UP
BROWNE_HCMV_INFECTION_2HR_DN
BROWNE_HCMV_INFECTION_2HR_UP
SONG_TARGETS_OF_IE86_CMV_PROTEIN
ZHU_CMV_24_HR_DN
Radiation
GHANDHI_DIRECT_IRRADIATION_UP
GHANDHI_BYSTANDER_IRRADIATION_UP
AMUNDSON_GAMMA_RADIATION_RESPONSE

SESTO_RESPONSE_TO_UV_C8
GENTILE_UV_RESPONSE_CLUSTER_D8
GENTILE_UV_RESPONSE_CLUSTER_D4
GENTILE_UV_RESPONSE_CLUSTER_D9
GENTILE_UV_LOW_DOSE_UP
GENTILE_UV_RESPONSE_CLUSTER_D5
GENTILE_UV_RESPONSE_CLUSTER_D7
DAZARD_UV_RESPONSE_CLUSTER_G1
SMIRNOV_RESPONSE_TO_IR_6HR_DN
ZHOU_CELL_CYCLE_GENES_IN_IR_RESPONSE_6HR
SMIRNOV_RESPONSE_TO_IR_2HR_DN
SMIRNOV_RESPONSE_TO_IR_2HR_UP
ZHOU_CELL_CYCLE_GENES_IN_IR_RESPONSE_2HR
P53
AMUNDSON_DNA_DAMAGE_RESPONSE_TP53
AMBROSINI_FLAVOPIRIDOL_TREATMENT_TP53
KEGG_P53_SIGNALING_PATHWAY
SCIAN_CELL_CYCLE_TARGETS_OF_TP53_AND_TP73_DN
WU_APOPTOSIS_BY_CDKN1A_VIA_TP53
KUMAMOTO_RESPONSE_TO_NUTLIN_3A_DN
KUMAMOTO_RESPONSE_TO_NUTLIN_3A_UP
BRCA and DNA repair
HONRADO_BREAST_CANCER_BRCA1_VS_BRCA2
PUJANA_BREAST_CANCER_WITH_BRCA1_MUTATED_UP
BAE_BRCA1_TARGETS_UP
MACLACHLAN_BRCA1_TARGETS_UP
PID_ATR_PATHWAY
E2F
OLSSON_E2F3_TARGETS_DN
CROSBY_E2F4_TARGETS
REN_BOUND_BY_E2F
EGUCHI_CELL_CYCLE_RB1_TARGETS
REACTOME_REGULATION_OF_MITOTIC_CELL_CYCLE
MOLENAAR_TARGETS_OF_CCND1_AND_CDK4_DN
VERNELL_RETINOBLASTOMA_PATHWAY_UP
Myc
SCHUHMACHER_MYC_TARGETS_UP
MENSSEN_MYC_TARGETS
COLLER_MYC_TARGETS_UP
SCHLOSSER_MYC_AND_SERUM_RESPONSE_SYNERGY
ODONNELL_TARGETS_OF_MYC_AND_TFRC_UP
COLLER_MYC_TARGETS_DN
KIM_MYC_AMPLIFICATION_TARGETS_DN
CEBALLOS_TARGETS_OF_TP53_AND_MYC_DN
SCHLOSSER_MYC_TARGETS_AND_SERUM_RESPONSE_DN
ODONNELL_TARGETS_OF_MYC_AND_TFRC_DN
DANG_REGULATED_BY_MYC_UP
EGF
AMIT_EGF_RESPONSE_120_HELA
AMIT_EGF_RESPONSE_480_MCF10A
AMIT_EGF_RESPONSE_20_HELA
ZWANG_EGF_INTERVAL_UP
NAGASHIMA_EGF_SIGNALING_UP
Aurora
PID_AURORA_B_PATHWAY
PID_AURORA_A_PATHWAY
OHASHI_AURKA_TARGETS
OHASHI_AURKB_TARGETS
Antigen presentation
REACTOME_ANTIGEN_PRESENTATION_FOLDING_ASSEMBLY_AND_PEPTIDE_LOADING_OF_CLASS_I_MHC
REACTOME_MHC_CLASS_II_ANTIGEN_PRESENTATION
KEGG_ANTIGEN_PROCESSING_AND_PRESENTATION
Metastasis
ZUCCHI_METASTASIS_UP
CHANDRAN_METASTASIS_TOP50_DN
RAMASWAMY_METASTASIS_UP
SUNG_METASTASIS_STROMA_UP
Multiple myeloma
CORRE_MULTIPLE_MYELOMA_UP
DAVIES_MULTIPLE_MYELOMA_VS_MGUS_DN
ZHAN_MULTIPLE_MYELOMA_PR_UP
RAS
SWEET_KRAS_TARGETS_UP
CHIARADONNA_NEOPLASTIC_TRANSFORMATION_KRAS_CDC25_DN
SWEET_KRAS_ONCOGENIC_SIGNATURE